

Epitaxy-induced structural phase transformations

Sverre Froyen, Su-Huai Wei, and Alex Zunger
Solar Energy Research Institute, Golden, Colorado 80401
 (Received 1 July 1988)

Using our calculated structural energies for CdTe, MgS, and NaCl, we describe how hydrostatic pressure versus volume data relate to epitaxial structural energies. We predict, e.g., that for thicknesses below a few monolayers CdTe may be grown in the β -Sn structure and MgS and NaCl can be stabilized in the zinc-blende form if grown on suitable substrates. Considerably thicker films may be grown metastably.

Structural phase transformations in solids are ordinarily achieved through changes in temperature or pressure. Since temperature effects are limited to energy differences $\sim k_B T$, yet many structures differ by more, pressure is often a better choice. Relative energy changes of more than 1 eV can be achieved through hydrostatic pressure in diamond anvils and even greater changes using shock waves. Since externally applied pressure normally must be positive, pressure-induced transformations can only realize phases with volumes smaller than that of the zero-pressure phase. Volume-increasing transformations such as from the dense $B1$ (rocksalt) to the open $B3$ (zincblende) structure are, therefore, impossible.

Effective pressure or stress can, however, also be applied by constraining a material inside or on a matrix of another solid. An epitaxially grown compound can offer such a system. If the material is grown coherently on a substrate with a different lattice parameter, the strain imposed by the substrate acts like a biaxial pressure. The strain can be positive or negative depending on whether the lattice parameter of the substrate is larger or smaller than that of the overlayer.

Apparent stabilization of unusual and even exotic structures through epitaxy is not new. Early observations include the growth of $B1$ cesium and thallium halides on mica and other substrates,¹ $B4$ (wurtzite) MgS and MgSe evaporated on alkali halides and metal films,^{2,3} and $B1$ InSb obtained by sputtering.⁴ More recently many metals that are normally fcc have been grown in the bcc structure,⁵⁻⁸ α -Sn has been grown outside its stable temperature range on InSb and CdTe substrates⁹ and an unusual rhombohedral SiGe has been grown on the (100) surface of Si.¹⁰ Some of the early examples may not have been stabilized through lattice coherence with the substrate; however, in many recent cases (the stabilization of bcc metals and α -Sn in particular) one observes a clear correlation between the substrate lattice constant and that of the pseudomorphic epitaxial phase.

This paper will focus on understanding the growth of compounds that are normally zinc-blende ($B3$) in the rocksalt ($B1$) structure and vice versa. For semiconductors, with the addition of the β -Sn analog ($A5$) and the hexagonal wurtzite ($B4$) phases, these are the likely low-energy structures.^{11,12} The $B1$ -to- $B3$ transition cannot be achieved by externally applied pressure and could expand the rather small known set of cubic, binary, fourfold coor-

inated compounds. Furthermore, since our calculations show that the direct band gap of a compound decreases when transforming from rocksalt to zinc-blende, it may increase the number of available semiconducting materials.

We will use the total energies of extended periodic solids to characterize epitaxial phases and transitions. Surface and interface effects are, therefore, neglected. These can be ignored provided the epitaxial layers are sufficiently thick; if surface energy differences are small, this assumption is valid even when comparing energies of thin layers. Assuming wetting¹³ and neglecting entropy effects, the stability of a coherent epitaxial overlayer is determined by its internal energy as a function of the substrate lattice constant. Using our calculated data for CdTe, shown in Figs. 1(a)-1(c), we now demonstrate how this function can be estimated from standard pressure versus volume data. Figure 1(a) shows the unit-cell volume versus applied external hydrostatic pressure; as pressure is increased CdTe undergoes two phase transformations: $B3$ to $B1$ to $A5$. Volume integration of the pressure data gives the energy as a function of volume for each phase (again under hydrostatic conditions). The offsets between energy minima of different phases (integration constants) are obtained from the transformation pressures through the common tangent constructions shown in Fig. 1(b).¹⁴ When a solid is constrained by coherent growth on a substrate, parallel to the interface the overlayer takes the lattice dimensions of the substrate. The appropriate external parameter for the energy is no longer pressure or volume, but rather the substrate lattice parameter(s), a_s . First, changing from a volume to an a_s representation involves structural geometric factors relating a_s to the cell volume V in different phases. With $a_s = \beta(V)^{1/3}$, we find

$$\beta_{B1} = \alpha 2^{1/6} = \beta_{B3},$$

$$\beta_{A5} = \alpha \left(\frac{2}{\eta} \right)^{1/3},$$
(1)

where $\eta(V)$ is the c/a ratio under hydrostatic conditions and α is a geometric scaling factor. The latter is needed since we make no assumptions about the detailed atomic structure at the interface and would, e.g., be used to describe the $\alpha = \sqrt{2}$ scaling when changing from a simple to

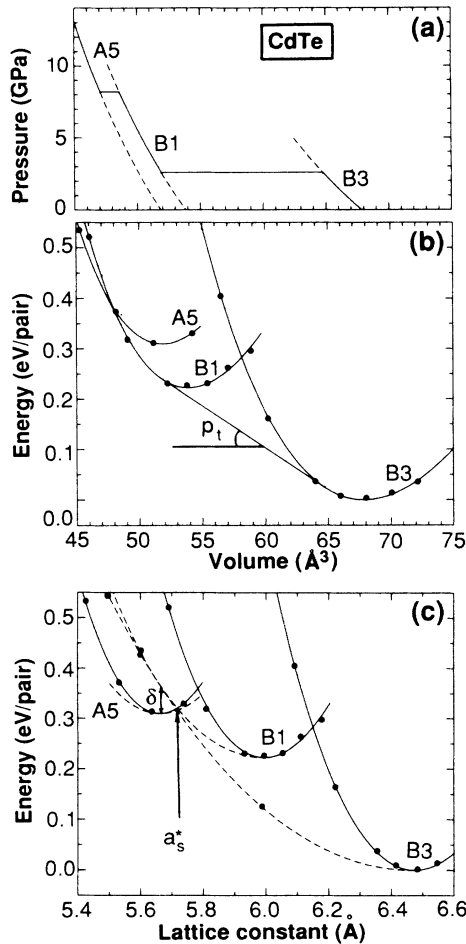


FIG. 1. Calculated structural energies for CdTe in the structures indicated. (a) and (b) are given under hydrostatic pressure conditions, while part (c) shows the energy as a function of (substrate) lattice parameter before (solid lines) and after (dashed line) c -axis relaxation. The epitaxial relaxation energy for $A5$ is estimated. We used $\alpha = \sqrt{2}$ for $B1$ and $B3$ and $\alpha = 1$ for the $A5$ phase [Eq. (1)].

a face-centered square lattice. Second, the unconstrained c axis, perpendicular to the interface, is free to relax. This reduces the energy of the epitaxial phase relative to the hydrostatically compressed phase evaluated at the same substrate lattice constant. Using second-order continuum elasticity theory,¹⁵ this energy reduction is determined from the elastic constants by minimizing the elastic energy with respect to c for fixed a_s . For cubic materials the ratio q of the relaxed epitaxial energy to the hydrostatic energy, both taken at the same a_s and referred to their common energy minimum, is

$$\begin{aligned}
 q_{[100]} &= \frac{2}{3} \left[1 - \frac{C_{12}}{C_{11}} \right], \\
 q_{[110]} &= \frac{1}{3} \frac{C_{11} - C_{12} + 6C_{44}}{C_{11} + C_{12} + 2C_{44}}, \\
 q_{[111]} &= \frac{4C_{44}}{C_{11} + 2C_{12} + 4C_{44}},
 \end{aligned} \quad (2)$$

where the subscripts refer to the growth direction. These two steps are illustrated for CdTe in Fig. 1(c). The solid lines show the energy as a function of a_s before c -axis relaxation and the dashed lines give the final epitaxial energy after relaxation. The epitaxial energies differ from the hydrostatic energies in Fig. 1(b) by (i) reduced elastic energies [Eq. (2)], causing a flattening of the curves and increasing the region of stability for the lowest-energy phase, and (ii) horizontal shifts of the energy minima [Eq. (1)]. The latter can separate two previously coinciding minima and expose an inaccessible phase, e.g., bcc ($\beta = 1.26$) and fcc ($\beta = 1.12$).¹⁶ These effects can result in qualitative changes in phase stability. Under hydrostatic pressure CdTe has two transitions: $B3$ to $B1$ and $B1$ to $A5$. Epitaxially, these are replaced by a single transition: $B3$ to $A5$. Relaxation of $B3$ leads to a situation where $B1$ is never a stable phase.

The existence of a competing phase with a lower energy minimum ($B3$) leads to a situation where nucleation of misfit dislocations can limit the thickness of the pseudomorphic phase ($A5$), even when the latter is lattice matched to the substrate. Selecting a substrate lattice matched to the $A5$ phase makes its energy independent of thickness. The competing $B3$ phase is higher in energy by δ [Fig. 1(c)]. However, the $B3$ film experiences a large misfit, and, once its critical thickness has been exceeded, it can lower its energy by nucleating misfit dislocations.¹⁷ The energy of the $B3$ phase will, therefore, decrease with increasing thickness, at some point dropping below the $A5$ phase. Then, $B3$ (with misfit dislocations) becomes the ground state, defining a critical thickness for the $A5$ phase.¹⁸ It is likely, however, that energy barriers will allow growth of much thicker metastable films than this equilibrium theory indicates. Note that, contrary to the situation in regular strained layer epitaxy, the critical thickness increases with the lattice mismatch. This is because it is the *competing* phase ($B3$) that experiences the misfit.

The above discussion permits prediction of systems likely to exhibit epitaxial phase transitions. For maximum stability enhancement δ , and hence, maximum critical thickness, we obtain three requirements. First, the difference between the minimum energies of the two competing phases should be small. A small transition pressure or a thermal transformation like α - to β -Sn may be an indication that this is satisfied. A second requirement is that the difference between the equilibrium lattice constants of the phases should be large. This may be satisfied by well-separated equilibrium volumes, such as the 20% volume difference between $B1$ and $B3$,^{11,12} or by different geometric factors [Eq. (1)], as for fcc and bcc.¹⁶ Finally, the lowest-energy, stable phase should be stiff, i.e., have a large bulk modulus as well as a large q ratio [Eq. (2)]. For anisotropic materials q depends on the growth direction. For cubic materials, Eq. (1) shows that if C_{44} is stiffer than the isotropic value, $\frac{1}{2}(C_{11} - C_{12})$ (as for most metals and semiconductors¹⁵) $q_{[111]}$ is the largest, whereas if C_{44} is softer (as it is for the alkali halides) $q_{[100]}$ is largest.

Energy differences between phases are often larger for semiconductors and insulators^{11,12} than for the $3d$ transi-

TABLE I. Static structural properties of CdTe, MgS, and NaCl in the indicated structures. a_0 is the equilibrium lattice constant, B_0 the bulk modulus, ΔE the minimum energy measured from the ground-state minimum, and E_c is the cohesive energy. All energies are per two atoms. The zero-pressure ground-state structure is indicated with an asterisk. CdTe and NaCl experimental lattice constants and bulk moduli are low-temperature values, all others are room-temperature values.

Structure			a_0 (Å)	B_0 (GPa)	ΔE (eV)	E_c (eV)
CdTe	$B3^*$	Theory	6.47	51	0	5.6
		Expt.	6.48 ^a	45 ^a		4.4 ^b
	$B1$	Theory	5.99	65	0.22	
	$A5$	Theory	5.66/3.23	69	0.31	
MgS	$B3$	Theory	5.59	61	0.17	
		Expt.	5.57 ^c			
	$B1^*$	Theory	5.13	82	0	8.8
		Expt.	5.20 ^d			8.0 ^b
NaCl	$B3$	Theory	6.14	22	0.26	
	$B1^*$	Theory	5.57	30	0	6.7
		Expt.	5.59 ^e	27 ^e		6.4 ^f

^aReference 26.

^bReference 27.

^cReference 3.

^dReference 28.

^eReference 29.

^fReference 15.

tion metals¹⁶ where epitaxial stabilization has been observed.^{5–8} Using Chelikowsky's empirical expansion of $B3$ to $B1$ transition pressures,¹⁹ as well as considering experimental pressure data,¹⁹ we have selected three compounds where a pseudomorphic phase might be stabilized through epitaxy: CdTe (normally $B3$), and MgS and NaCl (normally $B1$). Other candidates are AgBr, AgCl, CaS, CaSe, and MgSe (normally $B1$), and AgI, CdSe, CuI, HgS, HgSe, and HgTe (normally $B3$). All these materials have transition pressures less than ~ 3 GPa in magnitude.

Semirelativistic local-density approximation²⁰ (LDA) calculations have been performed to obtain structural energies under hydrostatic and (001) epitaxial conditions.

TABLE II. Differences ΔE (in eV) of band energies (Ref. 30) between the $B1$ and $B3$ phases and deformation potentials a (in meV/GPa) at selected symmetry points (origin at anion).

Structure		Γ_{1c}	X_{1c}	X_{3c}	L_{1c}
CdTe	ΔE_{B1-B3}	0.37	-3.45	2.27	1.49
	a_{B3}	62	-44	-3	20
	a_{B1}	107	9	-7	12
NaCl	ΔE_{B1-B3}	0.43	0.69	-1.09	3.39
	a_{B3}	101	17	64	126
	a_{B1}	151	96	-31	64
MgS	ΔE_{B1-B3}	0.48	-0.97	-1.37	-0.56

The linearized augmented plane-wave method²¹ was used for CdTe and NaCl, and the momentum space, pseudopotential method including stress calculation^{22–25} was used for MgS. Table I summarizes our results for ground-state structural properties compared to available experiment.^{3,26–29} Since elastic constants for MgS appear not to have been measured, our calculation, giving $C_{11} = 164$ GPa and $C_{12} = 40$ GPa, can be taken as a prediction. Figure 1(a) gives calculated transition pressures and volumes for CdTe.

Table II shows calculated shifts in electronic energy levels and their pressure derivatives. In all cases the lowest direct gap (at Γ) is smaller in the $B3$ than in the $B1$ phase. For CdTe, the X_{1c} state drops when transforming from $B3$ to $B1$, making the $B1$ phase metallic.

Figures 2 and 3 show results for NaCl and MgS corresponding to Fig. 1(c) for CdTe. We also show the relaxed c/a ratio. All $B3$ phases have very soft shear moduli $C_{11} - C_{12}$, leading to an extreme flattening (small q) of the epitaxial energy curves. Indeed, we find that under hydrostatic conditions $B3$ NaCl is unstable with respect to tetragonal deformation. Figure 2 shows that the substrate lattice parameter for epitaxial $B1$ to $B3$ crossover, $a_s^* = 6.5$ Å, lies to the right of the undistorted $B3$ minimum, which, therefore, cannot be reached. However, it may be possible to achieve a distorted $B3$ phase, with $c/a < 1$, by choosing $a_s > 6.5$ Å. Figure 3 shows that the $B3$ -phase minimum of MgS is accessible: The epitaxial energies cross at $a_s^* = 5.5$ Å. Using Matthews theory¹⁷ for misfit dislocations with our considerations above, we estimate the critical thickness for stable $B3$ MgS to be

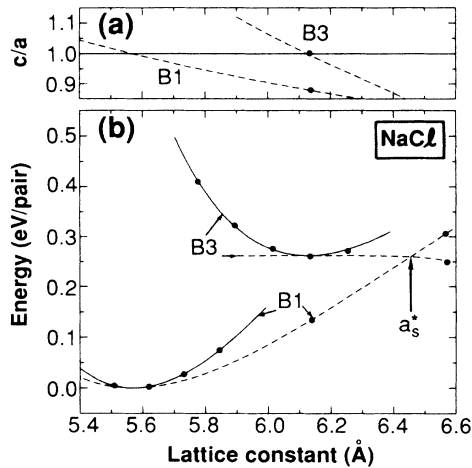


FIG. 2. Calculated structural energy and c/a ratios for $B1$ and $B3$ NaCl as a function of (substrate) lattice parameter. Solid and dashed lines show the energy before and after c -axis relaxation, respectively.

$\sim 5 \text{ \AA}$ for a_s at the $B3$ minimum, increasing to $\sim 9 \text{ \AA}$ if a_s is increased by 2%. Thicker layers may be grown metastably. Some substrates which are lattice matched to $B3$ MgS are BeTe, MnS, AlAs, and GaAs (all $B3$).

In conclusion, we have shown that coherent epitaxial growth away from lattice-matched conditions can lead to

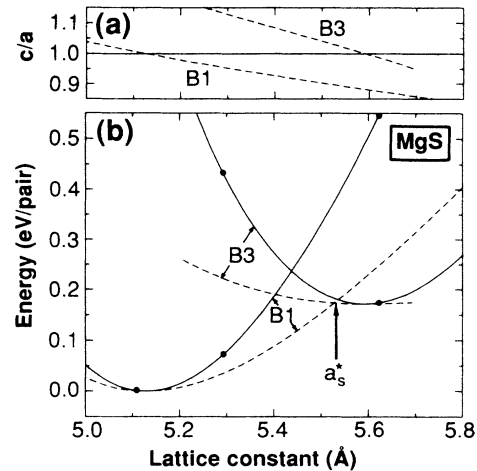


FIG. 3. Calculated structural energy and c/a ratios for $B1$ and $B3$ MgS as a function of (substrate) lattice parameter. Solid and dashed lines show the energy before and after c -axis relaxation, respectively.

stabilization of phases normally not accessible by pressure ($B3$ NaCl and MgS), and to destabilization or displacement of one phase by another ($B3$ and $A5$ CdTe).

We thank D. M. Wood and A. E. Blakeslee for helpful comments and suggestions.

¹L. G. Schulz, *J. Chem. Phys.* **18**, 996 (1950).

²G. Berthold, *Z. Phys.* **181**, 333 (1964).

³H. Mittendorf, *Z. Phys.* **183**, 113 (1965). The lattice constant of the $B3$ phase was calculated assuming the same cell volume as in the observed $B4$ (wurtzite) phase.

⁴S. Minomura, O. Shimomura, K. Asaumi, H. Oyanagi, and K. Takemura, in *Proceedings of the Seventh International Conference on Amorphous and Liquid Semiconductors*, edited by W. E. Spear (Center for Industrial Consultancy and Liaison, Univ. of Edinburgh, Edinburgh, Scotland, 1977), p. 53.

⁵G. A. Prinz, *Phys. Rev. Lett.* **54**, 1051 (1985).

⁶B. Heinrich, A. S. Arrott, J. F. Cochran, C. Liu, and K. Myrtle, *J. Vac. Sci. Technol. A* **4**, 1376 (1986).

⁷Z. Q. Wang, S. H. Lu, Y. S. Li, F. Jona, and P. M. Marcus, *Phys. Rev. B* **35**, 9322 (1987).

⁸Z. Q. Wang, Y. S. Li, F. Jona, and P. M. Marcus, *Solid State Commun.* **61**, 623 (1987).

⁹R. F. C. Farrow, *J. Vac. Sci. Technol. B* **1**, 222 (1983).

¹⁰A. Ourmazd and J. C. Bean, *Phys. Rev. Lett.* **55**, 765 (1985).

¹¹M. T. Yin and M. L. Cohen, *Phys. Rev. B* **26**, 5668 (1982).

¹²S. Froyen and M. L. Cohen, *Phys. Rev. B* **28**, 3258 (1983).

¹³R. Bruinsma and A. Zangwill, *Europhys. Lett.* **4**, 729 (1987).

¹⁴We obtained Fig. 1(a) by differentiating Fig. 1(b).

¹⁵C. Kittel, *Introduction to Solid State Physics*, 4th ed. (Wiley, New York, 1971).

¹⁶F. Jona and P. M. Marcus, in *The Structure of Surfaces II*, edited by J. F. van der Veen and M. A. Van Hove (Springer-Verlag, Berlin, 1988), p. 90. These authors have used $q = 1$, neglecting the differences between hydrostatic and epitaxial

energies.

¹⁷J. W. Matthews, in *Dislocations in Solids*, edited by F. R. N. Nabarro (North-Holland, Amsterdam, 1979), p. 461.

¹⁸For a_s around the $A5$ minimum, Matthew's theory gives a critical thickness less than the Burgers vector.

¹⁹J. R. Chelikowsky, *Phys. Rev. B* **35**, 1174 (1987).

²⁰Three different correlations were used: Hedin-Lundqvist for CdTe, Ceperley-Alder for MgS, and Wigner for NaCl.

²¹S.-H. Wei and H. Krakauer, *Phys. Rev. Lett.* **55**, 1200 (1985), and references therein.

²²J. Ihm, A. Zunger, and M. L. Cohen, *J. Phys. C* **12**, 4409 (1979).

²³G. Kerker, *J. Phys. C* **13**, L189 (1980).

²⁴S. G. Louie, S. Froyen, and M. L. Cohen, *Phys. Rev. B* **26**, 1738 (1982).

²⁵O. H. Nielsen and R. M. Martin, *Phys. Rev. B* **32**, 3780 (1985).

²⁶R. Dornhaus and G. Nimitz, in *Narrow-Gap Semiconductors*, edited by G. Hohler (Springer-Verlag, Berlin, 1983), p. 119.

²⁷O. Kubachewski and C. B. Alcock, *Metallurgical Thermochemistry*, 5th ed. (Pergamon, Oxford, 1979).

²⁸R. W. G. Wyckoff, *Crystal Structures*, 2nd ed. (Interscience, New York, 1963), Vol. 1.

²⁹J. T. Lewis, A. Lehoczy, and C. V. Briscoe, *Phys. Rev.* **161**, 877 (1967).

³⁰We calculate direct LDA gaps at Γ of 0.48, 4.01, 4.90 eV for CdTe ($B3$), MgS ($B1$), and NaCl ($B1$), respectively. Other gaps are 2.42, 2.76, and 7.18 for X_{1c} , 2.53, 4.22, and 7.52 for X_{3c} , and 1.60, 4.57, and 10.55 for L_{1c} .